IT Journal Research and Development (ITJRD)
Vol.9, No.2, March 2025, E-ISSN : 2528-4053 | P-ISSN : 2528-4061
DOI : 10.25299/itjrd.2025.17867

CNN-based Classification of Bladder Tissue Lesions from Endoscopy Images

Lutviana[1], Rian Ardianto[2], Purwono[3]
Departement of Informatics, Harapan Bangsa University[1,2,3]
luthvianna41@gmail.com[1], rianardianto@uhb.ac.id[2], purwono@uhb.ac.id[3]

Article Info

Article history:

Received Jun 30, 2024
Revised Oct 13, 2024
Accepted Mar 3, 2025

Keyword:

Bladder cancer
lesion classification
Convolutional Neural Network
Endoscopic image

ABSTRACT

Bladder cancer is one type of tumor that frequently occurs in the urinary system, and early diagnosis is essential to improve the prognosis and survival of patients. The study aims to develop a Convolutional Neural Network (CNN) model for bladder tissue lesion classification from endoscopic images. This study uses a dataset consisting of 1754 images, which are divided into four classes: High-Grade Cancer (HGC), Low-Grade Cancer (LGC), Non-Specific Tissue (NST), and Non-Tumorous Lesion (NTL). The proposed CNN model showed a validation accuracy of 96.29%, with high recall, precision, and F1-score in most classes. The results show that CNN-based automated methods can improve efficiency and accuracy in the early diagnosis of bladder cancer, reduce manual visual interpretation errors, and improve the quality of patient care. This study suggests increasing the training data, especially for the NTL class, and applying more complex model architecture to better results.

Corresponding Author:

Lutviana
Departement of Informatics
Harapan Bangsa University
Jl. KH. Wahid Hasyim No.274-A, Windusara, Karangklesem, Banyumas, Indonesia
Email: luthvianna41@gmail.com

1. INTRODUCTION

Health is an aspect that cannot be ignored because a healthy body is the key to preventing disease attacks [1]. Delayed diagnostics or inappropriate treatment can worsen a patient's illness, especially in the case of serious diseases such as potentially fatal cancers. Bladder cancer is one of the most common types of cancer worldwide and one of the leading causes of death with incidence rates increasing over time [2]. In a previous study [3], [4], it was mentioned that Bladder Cancer is one of the most common types of tumors in the urinary system.

Bladder cancer is the most common type of malignant tumor occurring in the urinary system, ranking tenth globally, with more cases occurring in men than in women [5]. According to global cancer statistics in 2018, Bladder Cancer (BC) ranked tenth as the most common type of cancer, with approximately 549,000 new cases diagnosed and 200,000 deaths reported annually [6]. Previous research mentions that based on clinicopathological characteristics, the incidence of bladder cancer is higher in men, older age groups, and smokers, which affects the survival rates [7].

The causes of BC are influenced by various factors, including genetic, environmental, and others. BC is highly associated with exposure to cigarette smoke [8] and occupational risks involving contact with chemicals such as certain aldehyde compounds, aluminum, benzidine and its

derivatives, and other compounds. Additionally, bladder infection by Schistosoma haematobium and mutations in the HRAS, Rb1, PTEN/MMAC1, NAT2, and GSTM1 genes also increase the risk of cancer. These mutations disrupt the regulatory functions of each gene [9].

A previous study [10] mentioned that in 2018, the Years of Life Lost (YLL) due to premature death caused by smoking-related cancer in Indonesia was 284,858.9 YLL. YLL is an indicator used to calculate the burden of a disease due to premature death. It was also stated that the ranking of YLL values for men was lung cancer (27,213), liver cancer (11,412), and bladder cancer (2,703.74). Early diagnosis and appropriate therapy are key to improving patient prognosis and survival rates [11], [12]. Early detection is crucial in increasing the chances of recovery and reducing the risk of complications. However, diagnosing bladder cancer often faces challenges due to its non-specific symptoms and the difficulty in accurately distinguishing between cancerous and non-cancerous lesions.

Diagnostic methods for bladder cancer often involve the use of endoscopic technology, particularly cystoscopy, which allows for direct visualization of the inside of the bladder. Cystoscopy is a medical procedure using a cystoscope to examine the urinary tract and bladder, assisting physicians in identifying potential lesions or tumors. The results of this procedure are digital images that must be interpreted by medical professionals. However, manual visual interpretation is often limited by human factors such as varying levels of expertise and limitations in visual perception. This can result in decreased diagnostic accuracy and increase the likelihood of errors in treatment recommendations. Therefore, the interpretation of medical images plays a crucial role in diagnosis and patient care, as errors in interpretation can significantly impact patient outcomes and prognosis [13].

As medical technology advances, the use of endoscopic imaging has become a primary choice for early detection and evaluation of bladder lesions. The main challenge in diagnosing bladder cancer is differentiating between high-grade and low-grade cancer, as well as distinguishing between cancerous and non-cancerous tissue. Convolutional Neural Networks (CNN) in endoscopic image analysis have been widely used due to their ability to classify images with high accuracy without the need for manual feature extraction. A previous study proposed a deep learning approach for bladder cancer detection and segmentation, combining CNN with a lightweight positional-encoding-free transformer and dual attention gates to enhance features through self and spatial attention. The method proposed in that study has proven to be computationally efficient, making it suitable for medical applications requiring real-time inference. The results showed that despite its compact architecture, the model is able to rival larger models in diagnostic accuracy [14].

CNN as a type of neural network has proven effective in various applications such as pattern recognition, natural language processing, computer-aided diagnosis, and computer image processing [15]. Table 1 summarizes recent studies that highlight the various approaches and results achieved in the classification and detection of bladder cancer.

Table 1. Previous Researches

Title	Author	Year	Method	Result
Multiclass Tissue Classification of Whole-Slide Histological Images using Convolutional Neural Networks	Rune Wetteland, dkk.	2019 [16]	Convolutional Neural Network (CNN)	The results show that the developed convolutional neural network (CNN) model has high accuracy in classifying urothelial carcinoma, with an average F1-score of 93.4% for six classes. This result reflects the model's ability to identify and distinguish important features in histological images, thus supporting more efficient and reliable cancer diagnosis, reducing pathologists' workload, and improving the quality of patient care.

Cystoscopic Image Classification by Unsupervised Feature Learning and Fusion of Classifiers	Seyyed Mohammad Reza Hashemi, dkk.	2021 [17]	Metode pre-trained convolutional neural network (CNN)	The proposed method achieved an accuracy of 69.02 ± 0.19 when classifying cystoscopy images into four categories: bloody urine, benign mass, malignant mass, and normal cases.
Sistem Pengembangan Deteksi Kanker Prostat Berbasis Image Processing dengan Metode Convolutional Neural Network	Alimin & Sigit Riyadi	2022 [18]	Convolutional Neural Network (CNN)	Identification of prostate cancer based on microscopic images of prostate cells by applying the Convolution Neural Network (CNN) method resulted in an accuracy rate of 93.3%.
Implementasi Algoritma Convolutional Neural Network Untuk Mendeteksi Penyakit Ginjal	Fahri Aulia Alfarisi Harahap, dkk.	2022 [19]	Convolutional Neural Network (CNN)	Normal kidney and cyst kidney images can be classified well by the model, but for tumor kidney and stone kidney sometimes misclassification can occur because the image of stone kidney and tumor kidney is very similar to cyst kidney. The final test accuracy result obtained from the entire training process is 75.17% with the f1-score accuracy of 68%.
Semi-Supervised Bladder Tissue Classification in Multi-Domain Endoscopic Images	Jorge F Lazo, dkk.	2023 [20]	Semi-supervised GAN based method	The proposed semi-supervised Generative Adversarial Network (GAN) based method achieves an overall average classification accuracy of 0.90, precision of 0.88, and recall of 0.89 for network classification in labeled domains (WLI).
Deep convolutional neural network accurately classifies different types of bladder cancer cells based on their pH fingerprints and morphology	Y. Belotti, dkk.	2023 [21]	CNN method with Inception-ResNet architecture	By combining pH imaging and deep learning, CNN accurately classified bladder cancer cell lines RT4 and J82 with a high accuracy of 99.4% for the testing dataset, showing a precision, gain, and F1 score of 98%.

This research aims to apply CNN to experiments with endoscopic images from public datasets. We classify bladder endoscopic images based on specific features, including High-Grade Cancer (HGC), Low-Grade Cancer (LGC), Non-Specific Tissue (NST), and Non-Tumorous Lesion (NTL), using a CNN model. The selection of the CNN model is based on its ability to mimic the human image recognition system, thus it is expected to improve efficiency and accuracy in classification, particularly in the healthcare context for classifying cancerous and non-cancerous bladder tissues.

2. RESEARCH METHOD

In conducting this research, several stages need to be completed. These stages aim to reduce errors in the research process. The research methodology flowchart is shown in Figure 1.

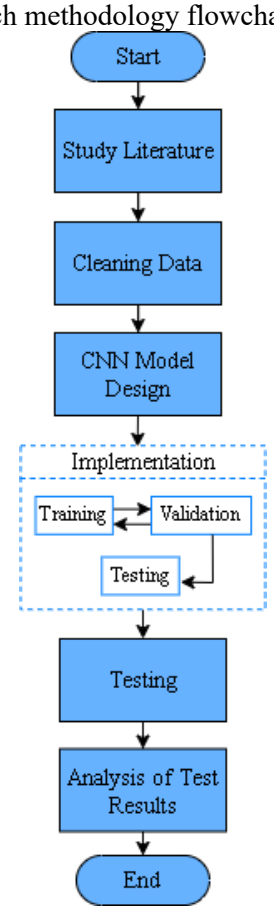

Figure 1. Research Method

2.1 Preparation Process

At this stage, preparation involves reviewing relevant literature related to the research topic. Another aspect of preparation is data collection. For this research, data collection utilizes an open-source dataset obtained from the Kaggle platform, specifically the Endoscopic Bladder Tissue Classification dataset (https://www.kaggle.com/datasets/aryashah2k/endoscopic-bladder-tissue-classification-dataset) [22]. This dataset contains 1,754 endoscopic images of bladder tissue with a total size of 241 MB, and a sample image from the dataset is shown in Figure 2. The research dataset includes four classes: HGC, LGC, NST, and NTL.

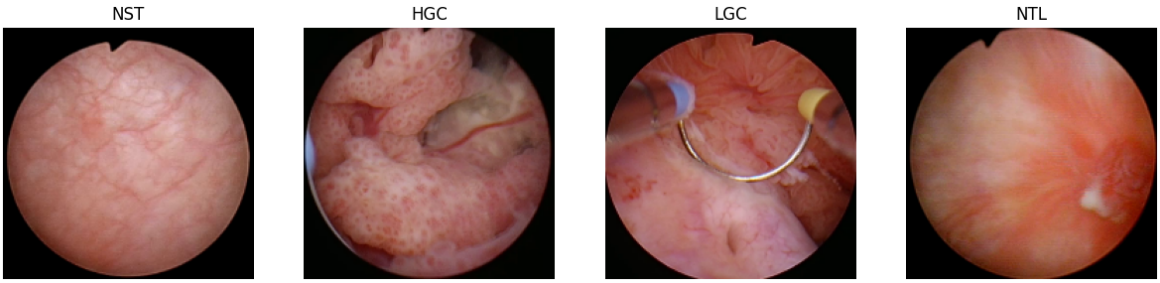

Figure 2. Sample Images of Bladder Tissue Types

2.2 Data Cleaning

The next stage is data cleaning, which involves the process of cleaning and preparing the data for use in model training. The dataset obtained from the Kaggle platform is processed through the following steps:

1. Data Count Check

The first step is to count the total number of images in the dataset to ensure that all images have been successfully downloaded and none are missing. This process confirms that all 1,754 images are available and ready for use in the research.

2. Loading Sample Images

   Several images from each class (HGC, LGC, NST, and NTL) are randomly loaded to verify that the images can be accessed correctly and that none are damaged or corrupted. This step is important to ensure the quality of the data used, as corrupted images can affect the model's training results.

3. Data Normalization

   All images in the dataset are normalized so that their pixel values fall within the range [0, 1]. Normalization is performed to help accelerate and stabilize the model training process. With normalization, the model can more easily handle variations in pixel intensity and achieve better convergence during training.

4. Dataset Splitting

   The dataset is divided into two subsets: training data and validation data. This division is done using stratified sampling to ensure that the proportion of each class is maintained in both subsets. Eighty percent of the dataset is used for training, while the remaining 20% is used for validation. This split is important for objectively evaluating the model's performance and avoiding overfitting.

5. Dataset Optimization

   To optimize performance during training, the dataset is cached and prefetching is performed. This step aims to reduce wait times during the training process by ensuring that data is always available for processing by the model. This technique uses available memory capacity to enhance the efficiency of the training process.

6. Data Visualization

   Images from each class are visualized to ensure that the data has been processed and categorized correctly. This visualization also serves as a final check before the data is used in the model training process. By examining the visual representations of the data, researchers can ensure that the class distribution is balanced and that each class is accurately represented in the dataset.

2.3 Model Building

At this stage, the architecture of the neural network model is designed to classify bladder tissue images into four classes: HGC, LGC, NST, and NTL. The model is built using the Keras Sequential API with several layers designed for feature extraction and classification.

The neural network model architecture is as follows:

1. Rescaling Layer: This layer is used to normalize the pixel values of the images to the range [0,1].
2. Convolutional Layers: There are three convolutional layers (Conv2D) with 16, 32, and 64 filters of size 3x3, each followed by a ReLU activation layer and a pooling layer (MaxPooling2D) to reduce the dimensionality of the features.
3. Flatten Layer: This layer is used to flatten the output from the last convolutional layer into a 1D vector.
4. Dense Layers: Two dense layers are used; the first has 128 neurons and uses ReLU activation, while the second has some neurons corresponding to the number of classes (4) and uses softmax activation for classification.

The model is then compiled using the Adam optimizer and the Sparse Categorical Cross entropy loss function, along with accuracy as the evaluation metric. The chosen architecture consists of three convolutional layers, which provide a balance between computational efficiency and feature extraction capability. More complex architectures such as ResNet or DenseNet were considered, but the simpler model was selected due to the relatively small dataset size and the need for a model that could achieve good performance with limited training time. While deeper architectures could offer potential accuracy improvements, they may also introduce overfitting, especially with smaller datasets, and require higher computational resources.

2.4 Implementation

The implementation is carried out using TensorFlow and Keras. The cleaned and prepared dataset is then used to train the model.

1. Dataset Splitting

   The dataset is divided into two parts: 80% for training and 20% for validation. This splitting is done stratified to ensure a balanced class proportion in both subsets.
2. Data Normalization

   The images in the dataset are normalized using a rescaling layer that converts pixel values from 0-255 to 0-1. This normalization is performed to accelerate and stabilize the training process.
3. Data Pipeline Optimization

   The dataset is cached and prefetched using the TensorFlow Data API to reduce wait times during training and ensure that data is always available for processing by the model.
4. Model Training

   The model is trained for 50 epochs using the training dataset, and the model's performance is evaluated on the validation dataset at the end of each epoch. Training is conducted using the backpropagation method with the Adam optimizer.

2.5 Testing

Testing is conducted by evaluating the model's performance on the validation dataset after the training process is completed. The evaluation is done by measuring accuracy and loss on the validation dataset. The evaluation results show the accuracy and loss achieved by the model during training. Additionally, the model is assessed using other classification metrics such as precision, recall, and F1-score. The model is used to predict labels on the validation dataset, and the predicted results are compared with the actual labels to generate a confusion matrix. The confusion matrix is visualized as a heatmap for further analysis.

2.6 The Analysis of the Test Results

The analysis of the test results is conducted to assess the model's performance in classifying bladder tissue images. Accuracy and loss during training and validation are plotted to observe trends and model performance. The accuracy and loss graphs indicate that the model achieves good convergence during training. The generated classification report shows metrics such as precision, recall, and F1-score for each class. These results provide a more detailed overview of the model's performance across classes and help identify classes that may require further attention.

The confusion matrix is used to analyze the model's performance in predicting each class. This matrix displays the number of correct and incorrect predictions for each class, facilitating the identification of classification errors. The model's prediction results are visualized with a heatmap of the confusion matrix to provide a visual representation of model performance. This visualization aids in understanding the distribution of predictions and the classification errors made by the model.

3. RESULTS AND ANALYSIS

This research utilizes an open-source dataset from Kaggle titled "Endoscopic Bladder Tissue Classification," consisting of 1,754 images. The entire dataset is used, which includes four classes: HGC, NST, LGC, and NTL. The dataset contains 469 images for the HGC class, 504 images for the NST class, 647 images for the LGC class, and 134 images for the NTL class.

The next step involves creating the CNN deep learning model. The model used in this research is implemented in Python using Google Colaboratory. The coding process requires several package libraries to facilitate computation, including TensorFlow, and for data visualization, the necessary libraries are Matplotlib and Seaborn.

Before proceeding to the model training phase, the data is separated into training and validation sets. The validation data is a portion of the dataset used to check whether the deep learning model can operate efficiently and correctly. In this testing phase, 20% of the total dataset per class is used for validation. The division of training and validation data is shown in Table 2.

Table 2. Data Splitting for Training and Validation

Class	Training Data	Validation Data
HGC	375	94
LGC	403	101
NST	518	129
NTL	107	27

The next stage is training the data. In deep learning, the training data is a collection of data used to train or build the model. The data used for training has image dimensions of 180x180 pixels and a batch size of 32. Matplotlib and Seaborn library packages are used to facilitate the visualization of the training data, allowing the displayed training data to be labeled for easier identification.

The following step is to build the model for classifying endoscopic images. In general, the CNN model consists of several modeling process steps, including convolution, pooling, flattening, and fully connected layers. The model filtering process is illustrated in Figure 3 and Table 3.

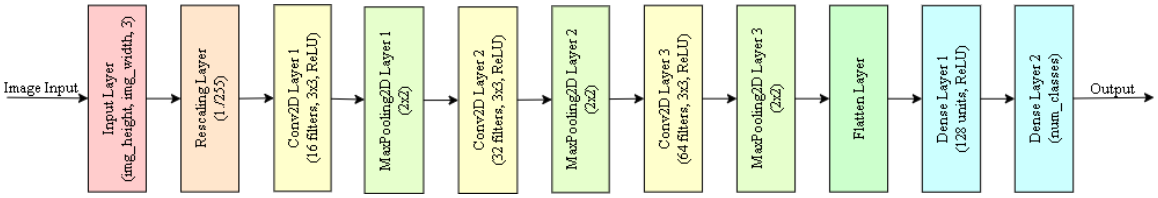

Figure 3. CNN Model

Table 3. CNN Model

Layer (type)	**Output Shape**	**Parameter #**
rescaling_1 (Rescaling)	(None, 180, 180, 3)	0
conv2d (Conv2D)	(None, 180, 180, 16)	448
max_pooling2d (MaxPooling2D)	(None, 90, 90, 16)	0
conv2d_1 (Conv2D)	(None, 90, 90, 32)	4640
max_pooling2d_1 (MaxPooling2D)	(None, 45, 45, 32)	0
conv2d_2 (Conv2D)	(None, 45, 45, 64)	18496
max_pooling2d_2 (MaxPooling2D)	(None, 22, 22, 64)	0
flatten (Flatten)	(None, 30976)	0
dense (Dense)	(None, 128)	3965056
dense_1 (Dense)	(None, 4)	516
Total Parameters		3989156
Trainable Parameters		3989156
Non-trainable Parameters		0

After defining the model architecture, the model is then compiled with the ‘Adam’ optimizer, ‘SparseCategoricalCrossentropy’ as the loss function, and ‘accuracy’ as the metric. The training process is conducted for 50 epochs. The training data is used to train the model to effectively classify the images. The results of the training data are presented in the graph shown in Figure 4.

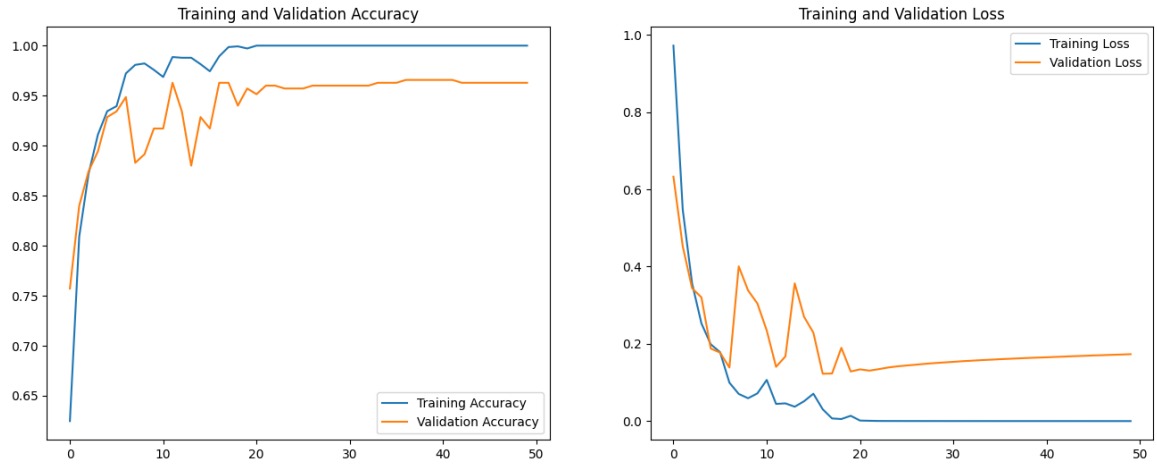

Figure 4. Accuracy and Loss (Training and Validation)

Based on the training results conducted over 50 epochs, both the training and validation results approach a value of 1. At epoch 50, the training accuracy achieved is 1.0000, while the validation accuracy (val_accuracy) is 0.9629. At this epoch, the loss value is 4.4272e-05 for training, and the validation loss (val_loss) is 0.1732.

The next step is to calculate the accuracy, precision, recall, and F1-score. These values are obtained from the confusion matrix. The confusion matrix is a table that contains information about the prediction results and actual values with four different combinations. It represents the classification results with four values: True Positive (TP), True Negative (TN), False Positive (FP), and False Negative (FN). The results of the validation test confusion matrix are shown in Figure 5.

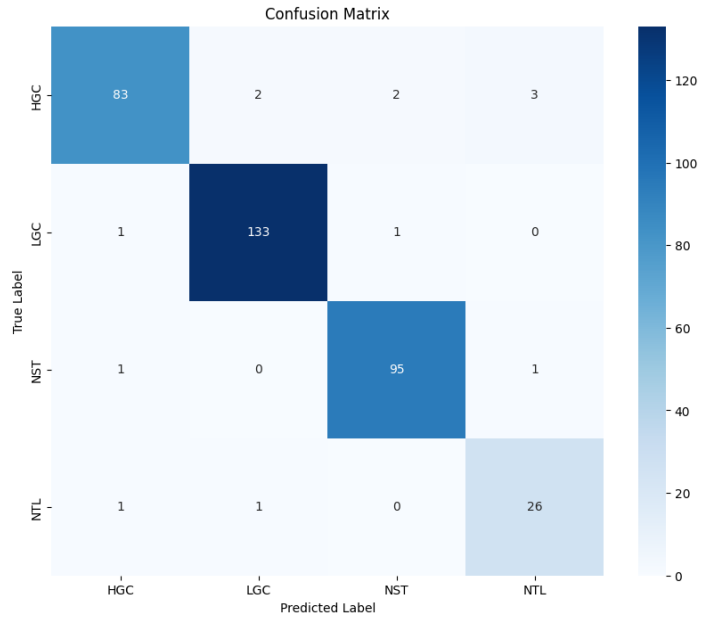

Figure 5. Confusion Matrix

From the confusion matrix above, there are several values resulting from the validation test, including True Positive (TP), False Negative (FN), False Positive (FP), and True Negative (TN) for each class. Here is the mathematical calculation for accuracy, precision, recall, and F1 score.

a. Accuracy. Accuracy represents how accurately a model classifies correctly and is calculated using the formula (1)

$$Accuracy = \frac{TP + TN}{TP + TN + FP + FN} \times 100\% \quad (1)$$

$$= \frac{83 + 133 + 95 + 26}{83 + 2 + 2 + 3 + 1 + 133 + 1 + 0 + 1 + 0 + 95 + 1 + 1 + 1 + 0 + 2683 + 133 + 95 + 26} \times 100\%$$

$$= \frac{337}{350} \times 100\% = 0.9629 \times 100\% = 96.29\%$$

b. Precision. Precision represents the accuracy of the predictions made by the model relative to the actual data, and is calculated using the formula (2).

$$Precision = \frac{TP}{TP + FP} \times 100\% \quad (2)$$

$$Precision\ (HGC) = \frac{83}{\mathbf{83} + 1 + 1 + 1} \times 100\% = \frac{83}{86} \times 100\% = 97\%$$

$$Precision\ (LGC) = \frac{133}{2 + 133 + 0 + 1} \times 100\% = \frac{133}{136} \times 100\% = 98\%$$

$$Precision\ (NST) = \frac{95}{2 + 1 + 95 + 0} \times 100\% = \frac{95}{98} \times 100\% = 97\%$$

$$Precision\ (NTL) = \frac{26}{3 + 0 + 1 + 26} \times 100\% = \frac{26}{30} \times 100\% = 87\%$$

c. Recall or Sensitivity. Recall describes the model's success in retrieving relevant information and is calculated using the formula (3).

$$Recall = \frac{TP}{TP + FN} \times 100\% \quad (3)$$

$$Recall\ (HGC) = \frac{83}{83 + 2 + 2 + 3} \times 100\% = \frac{83}{90} \times 100\% = 92\%$$

$$Recall\ (LGC) = \frac{133}{1 + 133 + 0 + 1} \times 100\% = \frac{133}{135} \times 100\% = 99\%$$

$$Recall\ (NST) = \frac{95}{1 + 0 + 95 + 1} \times 100\% = \frac{95}{97} \times 100\% = 98\%$$

$$Recall\ (NTL) = \frac{26}{1 + 1 + 0 + 26} \times 100\% = \frac{26}{28} \times 100\% = 93\%$$

d. F-1 Score. The F-1 score represents the weighted average of precision and recall and is calculated using the formula (4).

$$F1 - Score = 2 \times \frac{precision \times recall}{precision + recall} \quad (4)$$

$$F1 - Score\ (HGC) = 2 \times \frac{97\% \times 92\%}{97\% + 92\%} = 94\%$$

$$F1 - Score\ (LGC) = 2 \times \frac{98\% \times 99\%}{98\% + 99\%} = 98\%$$

$$F1 - Score\ (NST) = 2 \times \frac{97\% \times 98\%}{97\% + 98\%} = 97\%$$

$$F1 - Score\ (NTL) = 2 \times \frac{87\% \times 93\%}{87\% + 93\%} = 90\%$$

From the mathematical calculations above, the model performance metrics are presented in Table 4.

Table 4. Model Performance Metrics

Class	Precision	Recall	F1-Score	Support
HGC	97%	92%	94%	90
LGC	98%	99%	98%	135
NST	97%	98%	97%	97
NTL	87%	93%	90%	28

After training the model, the evaluation results on the validation dataset show that the model achieved a validation accuracy of 96.29%. Overall, the model's accuracy reached 96%, with average precision, recall, and F1-score values of 95% for macro average and 96% for weighted average.

The imbalance in the number of data between the NTL class and the other classes seems to contribute to the model's decreased performance in classifying non-tumorous lesions. With only 134 images for the NTL class compared to more than 400 images for the other classes, the model may struggle to learn representative patterns from the NTL class. As a result, the precision, recall, and f1-score values for the NTL class are lower than those for the other classes, at 87%, 93%, and 90%, respectively, indicating that the model tends to make more mistakes in distinguishing this class from others.

Several approaches can be taken to address this imbalance issue, such as using oversampling techniques or data augmentation to increase the number of images in the NTL class or applying a class-weighted loss function to give more weight to errors occurring in the NTL class during training. Another alternative is to use focal loss, which is designed to handle data imbalance by focusing on errors from minority classes. Implementing these solutions is expected to improve the model's ability to more accurately recognize patterns in non-tumorous lesions. While these techniques were not implemented in this study, they represent potential strategies for addressing the class imbalance issue in future research.

The confusion matrix in Figure 5. provides a more detailed view of the prediction errors. For example, there are some misclassifications where HGC tissue is classified as NTL and vice versa. These errors may be caused by the visual similarity between these tissues or possibly by the limitations of the training data available for the NTL class.

This custom CNN model demonstrates advantages in terms of simplicity and computational speed due to its lighter architecture. However, to further enhance performance, several steps can be taken, such as adding more training data, especially for the NTL class, or exploring more complex model architectures.

Table 5. Comparison with previous research

Title	Author	Year	Method	Accuracy
Multiclass Tissue Classification of Whole-Slide Histological Images using Convolutional Neural Networks	Rune Wetteland, dkk. [16]	2019	Convolutional Neural Network (CNN)	93.4%

Cystoscopic Image Classification by Unsupervised Feature Learning and Fusion of Classifiers	Seyyed Mohammad Reza Hashemi, dkk. [17]	2021	Metode pre-trained convolutional neural network (CNN)	69,02% ± 0,19
Sistem Pengembangan Deteksi Kanker Prostat Berbasis Image Processing dengan Metode Convolutional Neural Network	Alimin & Sigit Riyadi [18]	2022	Convolutional Neural Network (CNN)	93,3%.
Implementasi Algoritma Convolutional Neural Network Untuk Mendeteksi Penyakit Ginjal	Fahri Aulia Alfarisi Harahap, dkk. [19]	2022	Convolutional Neural Network (CNN)	75,17%
Semi-Supervised Bladder Tissue Classification in Multi-Domain Endoscopic Images	Jorge F Lazo, dkk. [20]	2023	Semi-supervised GAN based method	90%
Klasifikasi Lesi Jaringan Kandung Kemih Berbasis CNN dari Citra Endoskopi	Lutviana, dkk.	2024	Metode Convolutional Neural Network (CNN) Custom	96.29%

4. CONCLUSION

In this research, a CNN-based model was developed to classify bladder tissue images into four classes: HGC, LGC, NST, and NTL. The model achieved an overall accuracy of 96%, demonstrating effective performance in identifying cancerous tissues. The precision, recall, and F1-score for the HGC, LGC, and NST classes were all above 90%, indicating the model's ability to accurately classify these classes. However, the model's performance was slightly lower for the NTL class, with a precision of 87% and a recall of 93%, largely due to the limited number of images in this class.

The results highlight the effectiveness of the proposed CNN architecture in classifying bladder cancer images, although the imbalanced dataset remains a challenge, particularly for the NTL class. Addressing this issue by incorporating advanced techniques such as oversampling, data augmentation, or using a class-weighted loss function could improve the model's ability to distinguish non-tumor lesions.

The potential practical application of this study lies in its contribution to automated cancer diagnosis, particularly in assisting pathologists with rapid and accurate bladder cancer classification. The CNN model could be integrated into clinical workflows, reducing the manual labor and potential human error associated with traditional diagnostic methods. However, the primary challenge in adopting this model for clinical practice lies in the need to address data imbalance issues, particularly for rare or less-represented classes like NTL. Moreover, further validation on larger and more diverse datasets will be essential to ensure the model's robustness and generalizability in real-world clinical settings. Additionally, the model may require optimization or adaptation to comply with clinical standards and regulatory requirements for medical device software.

This study provides a basis for further research in bladder cancer classification using deep learning techniques. Future studies could focus on enhancing model performance for underrepresented classes by utilizing more complex architectures or techniques aimed at mitigating data imbalance, which could lead to more accurate and reliable classification results. By overcoming these challenges, the model holds the potential to significantly streamline and improve bladder cancer diagnostics in clinical practice.

REFERENCES

[1] M. Muharrom, “Klasifikasi Diagnosa Peradangan Kandung Kemih Menggunakan Metode Algoritma Naïve Bayes,” *Indonesian Journal of Business Intelligence (IJUBI)*, vol. 3, no. 2, p. 31, Jan. 2021, doi: 10.21927/ijubi.v3i2.1472.

[2] D. Sugeng Supriyadi, D. Wanadi, and H. Setyono, "Prosedur Terapi Radiasi Eksterna pada Pasien Kanker Kandung Kemih dengan Metastasis Articulatio Coxae," *JRI (Jurnal Radiografer Indonesia)*, vol. 4, no. 2, pp. 82–85, Nov. 2021, doi: 10.55451/jri.v4i2.93.

[3] J. Li, C. Cheng, and J. Zhang, "Autoimmune diseases and the risk of bladder cancer: A Mendelian randomization analysis," *J Autoimmun*, vol. 146, p. 103231, Jun. 2024, doi: 10.1016/j.jaut.2024.103231.

[4] X. Dong *et al.*, "Clinical practice guideline on bladder cancer (Part I)," *UroPrecision*, vol. 1, no. 1, pp. 20–30, Mar. 2023, doi: 10.1002/uro2.11.

[5] S. Kural, G. Jain, S. Agarwal, P. Das, and L. Kumar, "Urinary extracellular vesicles-encapsulated miRNA signatures: A new paradigm for urinary bladder cancer diagnosis and classification," *Urologic Oncology: Seminars and Original Investigations*, Apr. 2024, doi: 10.1016/j.urolonc.2024.03.006.

[6] T. Nohara *et al.*, "Variations in photodynamic diagnosis for bladder cancer due to the quality of endoscopic equipment," *Photodiagnosis Photodyn Ther*, vol. 37, p. 102628, Mar. 2022, doi: 10.1016/j.pdpdt.2021.102628.

[7] I. Anwar *et al.*, "Prevalence and survival in patients with bladder cancer: a study in high cancer incidence zone," *Asian Pacific Journal of Health Sciences*, vol. 9, no. 4, pp. 243–247, Jun. 2022, doi: 10.21276/apjhs.2022.9.4.48.

[8] K. Vaidya, O. Vijayanand Potdar, P. Charuchandra Bhide, and A. Vikram Patkar, "Clinico-pathological Profile of Bladder Cancer Patients in A Tertiary Care Centre," *Int J Sci Res*, pp. 41–44, Apr. 2023, doi: 10.36106/ijsr/0701547.

[9] L. Dzakiyyah Zulfa, D. Salim, and A. Tirza Melia Silalahi, "Potensi ncRNA dan lncRNA Dalam Diagnosis Kanker kandung Kemih Non Invasif," *Cerdika: Jurnal Ilmiah Indonesia*, vol. 1, no. 4, pp. 384–391, Apr. 2021, doi: 10.59141/cerdika.v1i4.52.

[10] P. R. Puspawati, S. A. Kristina, and C. Wiedyaningsih, "Dampak Merokok Terhadap Kematian Dini Akibat Kanker di Indonesia: Estimasi Years of Life Lost (YLL)," *Majalah Farmaseutik*, vol. 16, no. 1, pp. 101–106, Sep. 2020, doi: https://doi.org/10.22146/farmaseutik.v16i1.49790.

[11] D. Waruwu and R. Rosnelly, "Deteksi Penyakit Kanker Kandung Kemih Berdasarkan Pengolahan Citra Digital," *Journal of Machine Learning and Data Analytics*, vol. 2, no. 1, pp. 1–5, Feb. 2023, [Online]. Available: https://journal.fkpt.org/index.php/malda/article/view/479

[12] R. Tryaka, "Faktor Prognostik terhadap Pemulihan Pasien Kanker Kandung Kemih Paska Operasi Radikal Sistektomi," Universitas Gadjah Mada, 2020.

[13] M. S. Devi, J. A. Pandian, D. Umanandhini, V. V, and V. G. P, "Endoscopic Bladder Tissue Classification Using Seventeen Layered Deep Convolutional Neural Network," in *2024 International Conference on Advancements in Smart, Secure and Intelligent Computing (ASSIC)*, IEEE, Jan. 2024, pp. 1–6. doi: 10.1109/ASSIC60049.2024.10507996.

[14] M. Amaouche, O. Karrakchou, M. Ghogho, A. El Ghazzaly, M. Alami, and A. Ameur, "Redefining Cystoscopy With AI: Bladder Cancer Diagnosis Using an Efficient Hybrid CNN-Transformer Model," in *2024 IEEE International Conference on Image Processing (ICIP)*, IEEE, Oct. 2024, pp. 3030–3036. doi: 10.1109/ICIP51287.2024.10647282.

[15] M. A. K. Raiaan *et al.*, "A systematic review of hyperparameter optimization techniques in Convolutional Neural Networks," *Decision Analytics Journal*, vol. 11, p. 100470, Jun. 2024, doi: 10.1016/j.dajour.2024.100470.

[16] R. Wetteland, K. Engan, T. Eftestøl, V. Kvikstad, and E. Janssen, "Multiclass Tissue Classification of Whole-Slide Histological Images using Convolutional Neural Networks," in *Proceedings of the 8th International Conference on Pattern Recognition Applications and Methods*, SCITEPRESS - Science and Technology Publications, 2019, pp. 320–327. doi: 10.5220/0007253603200327.

[17] S. M. R. Hashemi, H. Hassanpour, E. Kozegar, and T. Tan, "Cystoscopic Image Classification by Unsupervised Feature Learning and Fusion of Classifiers," *IEEE Access*, vol. 9, pp. 126610–126622, 2021, doi: 10.1109/ACCESS.2021.3098510.

[18] Alimin and S. Riyadi, "Sistem Pengembangan Deteksi Kanker Prostat Berbasis Image Processing dengan Metode Convolutional Neural Network," *Explore IT : Jurnal Keilmuan dan Aplikasi Teknik Informatika*, vol. 14, no. 2, pp. 52–63, Dec. 2022, doi: https://doi.org/10.35891/explorit.v14i2.3535.

[19] F. A. A. Harahap, R. M. Sinaga, K. Arifin, and K. S. S, "Implementasi Algoritma Convolutional Neural Network Untuk Mendeteksi Penyakit Ginjal," *Jurnal Teknologi Informasi, Komputer dan Aplikasinya (JTIKA*, vol. 4, no. 2, pp. 212–219, Sep. 2022, doi: https://doi.org/10.29303/jtika.v4i2.202.

[20] J. F. Lazo *et al.*, "Semi-Supervised Bladder Tissue Classification in Multi-Domain Endoscopic Images," *IEEE Trans Biomed Eng*, vol. 70, no. 10, pp. 2822–2833, Oct. 2023, doi: 10.1109/TBME.2023.3265679.

[21] Y. Belotti, D. S. Jokhun, V. L. M. Valerio, T. W. Chong, and C. T. Lim, "Deep convolutional neural network accurately classifies different types of bladder cancer cells based on their pH fingerprints and morphology," *AIP Adv*, vol. 13, no. 5, May 2023, doi: 10.1063/5.0120216.
[22] J. F. Lazo *et al.*, "Endoscopic Bladder Tissue Classification Dataset," Zenodo.